




# Strong pinning at high growth rates in rare earth barium cuprate (REBCO) superconductor films grown with liquid-assisted processing (LAP) during pulsed laser deposition

J Feighan<sup>1</sup> , M H Lai<sup>1</sup>, A Kursumovic<sup>1</sup>, D Zhang<sup>2</sup>, H Wang<sup>2</sup> , J H Lee<sup>3</sup>, S Moon<sup>3</sup> and J L MacManus-Driscoll<sup>1</sup> 

<sup>1</sup> Department of Materials Science and Metallurgy, University of Cambridge, 27 Charles Babbage Road, Cambridge CB3 0FS, United Kingdom

<sup>2</sup> School of Materials Engineering, Purdue University, 701 West Stadium Avenue, West Lafayette, IN 47907-2045, United States of America

<sup>3</sup> SuNAM, 52 Seungnyang-gil, Wongok-myeon, Anseong-si, Gyeonggi-do 17554, Republic of Korea

E-mail: [jff2@cam.ac.uk](mailto:jff2@cam.ac.uk)

Received 16 November 2020, revised 15 January 2021

Accepted for publication 29 January 2021

Published 25 February 2021



## Abstract

We present a simple liquid-assisted processing (LAP) method, to be used *in situ* during pulsed laser deposition growth to give both rapid growth rates (50 Hz deposition leading to  $>250 \text{ nm min}^{-1}$  with a single plume) and strong pinning (improved  $\times 5\text{--}10$  at 30 K and below, over plain standard YBCO films grown at similar rates). Achieving these two important features *simultaneously* has been a serious bottleneck to date and yet for applications, it is critical to overcome it. The new LAP method uses a non-stoichiometric target composition, giving rise to a small volume fraction of liquid phase during film growth. LAP enhances the kinetics of the film growth so that good crystalline perfection can be achieved at up to  $60\times$  faster growth rates than normal, while also enabling artificial pinning centres to be self-assembled into fine nanocolumns. In addition, LAP allows for RE mixing (80% of Y with 20% of Yb, Sm, or Yb + Sm), creating effective point-like disorder pinning centres within the rare earth barium cuprate lattice. Overall, LAP is a simple method for use in pulsed laser deposition, and it can also be adopted by other *in situ* physical or vapour deposition methods (i.e. MOCVD, evaporation, etc) to significantly enhance both growth rate and performance.

Supplementary material for this article is available [online](#)

Keywords: pinning, liquid-assisted, REBCO

(Some figures may appear in colour only in the online journal)



Original content from this work may be used under the terms of the [Creative Commons Attribution 4.0 licence](#). Any further distribution of this work must maintain attribution to the author(s) and the title of the work, journal citation and DOI.

## 1. Introduction

(Rare-earth)Ba<sub>2</sub>Cu<sub>3</sub>O<sub>7-x</sub> or rare earth barium cuprate (REBCO) coated conductors have the potential to revolutionise multiple power and high field magnet applications [1, 2]. However, despite great advances in coated conductor technology over the past 25 years, achieving high in-field performance and low cost simultaneously still remains challenging [3]. Of particular importance is mid-field (3–10 T) applications working at low temperatures (20 K–30 K), including generators for wind turbines, motors, etc. Standard vapour-grown REBCO films can deliver good performance in this region but growth rates are relatively slow and yields are uncertain. A reliable method for fast growth, with high yield, giving strong pinning is needed. The higher the supersaturation the process, the better in terms of yield and uniformity, and pulsed laser deposition (PLD) is the best process in that regard. If speeds of PLD could be increased, while maintaining strong performance, then costs will come down. The question is how to achieve this goal.

Higher speed growth can be achieved via the use of liquid-assisted methods owing to the faster growth kinetics. The first liquid growth method used to produce REBCO was via a method called liquid phase epitaxy (LPE) [4–6], initially developed by the semiconductor industry to grow III–V, II–VI and IV–VI compounds for various device applications. e.g. the GaAs/GaAlAs double-heterostructure laser diode [7]. When used to grow REBCO, it was shown to enable growth rates at least  $\times 50$  higher than standard [8]. However, LPE is not an industrially practical process owing to the need for a large volume of the highly reactive Ba-Cu-O molten liquid precursor and its reactions with the substrate.

Later on, the hybrid LPE (HLPE) method was developed and this had the advantage of being able to use standard thin film growth equipment, rather than a large crucible of liquid. In it a thin liquid layer ( $\sim 1 \mu\text{m}$ ) is initially deposited on the substrate [9, 10], after which vapour species are delivered to the liquid surface, supersaturating it, and forcing REBCO to crystallize out onto the substrate surface. The REBCO formation rate is high (as in LPE) owing to the much enhanced diffusion rates of RE species in liquid compared to surface diffusion rates on a substrate surface. Growth rates of  $500 \text{ nm min}^{-1}$  and self-field  $J_c$ 's over  $1 \text{ MA cm}^{-2}$  in  $3 \mu\text{m}$  thick films at 77 K [11] are achievable. However, the process has the disadvantage of being two-step, with the liquid layer needing to be deposited before the REBCO growth step. Also, the process has intrinsically lower supersaturation than other standard vapour processes, requiring careful control of the processing to produce high performance films. A third liquid process, with industrial success, is the process developed by SuNAM [12] which is based on *ex-situ* liquid processing. It has an extremely fast conversion rate (over  $100 \text{ nm s}^{-1}$ ) [13] and involves the deposition of an amorphous non-stoichiometric RE-Ba-Cu-O film, followed by conversion, *ex-situ*, to REBCO via a liquid after increasing the temperature and  $pO_2$  sequentially [12]. The process gives very high  $J_c$  ( $3.2 \text{ MA cm}^{-2}$ ) conductors at 77 K in self-field [13, 14], although currently films produced by this method suffer from the creation of relatively large Gd<sub>2</sub>O<sub>3</sub>

particles that are embedded within the REBCO matrix. These particles are too large to be effective pinning centres for high field applications [14].

To achieve the aforementioned goals of high performance at fast growth rates, we have developed a new process termed liquid-assisted processing (LAP). LAP is a simple *in situ* process in which a non-stoichiometric target is used to deposit thin films. The composition is selected so that during growth a small ( $\sim 6 \text{ vol.}\%$ ) liquid fraction forms, allowing for faster diffusion of the deposited species in the film. The method is expected to be adaptable to a wide range of physical or chemical vapour deposition processes.

This work is aimed at producing films for applications where high critical currents ( $> \sim 1000 \text{ A}$ ) can be achieved in fields above 5 T which means operating at  $\sim 30 \text{ K}$  or below. It is also aimed at lower cost conductor. This necessitates creating films at fast growth rates with very strong pinning centres engineered into them. To achieve fast growth rates, the presence of liquids during growth is highly beneficial. To achieve strong pinning in the field range of interest, different pinning morphologies need to be engineered into the films, notably extended 1D (columnar) artificial pinning centres (APCs) and 0D-like (point defects) [15].

As far as point pinning defects goes, we hypothesise that they will be created by using mixed rare-earths REBCO films, i.e. using at least two REs of different atomic sizes to create RE<sub>1-x</sub>RE<sub>2x</sub>BCO films [3]. The difference in the size of the RE ions (ion size variance) [16] leads to localised regions of strain within the lattice which can potentially act as pinning sites [16, 17]. Additionally, for rare-earth ions of a similar size to the Ba<sup>2+</sup> ion, Ba-RE cross substitution occurs creating further point defects [18, 19].  $x$  needs to be small in RE<sub>1-x</sub>RE<sub>2x</sub>BCO so that the growth temperature can be optimised for RE1. If  $x$  is large then the growth temperature would not be optimised for either RE1 or RE2 and this would lead to poor overall crystallinity and likely irregular buckling of the CuO planes, both being detrimental to superconductivity.

Samples with a mixed rare-earth component have been shown to have mildly improved performance at 77 K [20–23]. However, it is at lower temperatures that such point defects are expected to be most beneficial, with previous studies predicting that they will become the major contribution to the vortex pinning force at low temperatures [24].

Overall, in this paper we demonstrate mixed RE, REBCO films made rapidly and *in situ* using a new, extremely fast LAP method, termed LAP. Films are grown with a range of pinning centres included point-like defects, columnar defects, and a mix of both types of defect. We demonstrate that films grown on single crystal substrates using this new method exhibit high  $J_c$  values, especially at low temperatures, and we discuss the enhanced performance in terms of the nanostructured defects present in the films.

## 2. Experimental

PLD targets were made from single phase powders of Y<sub>2</sub>O<sub>3</sub>, Ba(NO<sub>3</sub>)<sub>2</sub>, CuO and, where needed, powders of Sm<sub>2</sub>O<sub>3</sub> and

$\text{Yb}_2\text{O}_3$ . All powders were weighed to the appropriate amounts, mixed by hand, ground, pressed and finally reacted at 850 °C in oxygen for 24 h. The targets were then re-ground and re-sintered to ensure homogeneity and that a complete reaction occurred. Seven different composition targets were made, as shown in table 1.

For mixed RE targets, the at. % of Y was always 80% so that the growth temperature could be kept the same for all films. To balance the 80 at. % Y, and hence ensure stoichiometry, we used 20% additions of the RE additives. We used rare-earths smaller ( $\text{Yb}^{3+}$ ), larger ( $\text{Sm}^{3+}$ ) or a combination of smaller and larger ( $\text{Yb}^{3+}$ ,  $\text{Sm}^{3+}$ ) than the matrix rare-earth ( $\text{Y}^{3+}$ ).

Two of the LAP films had 5 mol. %  $\text{Ba}_2\text{YNbO}_6$  (BYNO) APCs added to them (table 1). One film was pure YBCO and the other a mixed RE film. BYNO was chosen as previous works showed that BYNO additions produce strong *c* axis pinning (up to twice the  $J_c$  for  $\text{H} \parallel c$  as compared to pure YBCO films [26]), even at relatively high growth rates ( $>1 \text{ nm s}^{-1}$ ). Hence, BYNO can self-assemble into nanocolumns at high growth rates where other APCs cannot [26, 27]. Since LAP is a fast process, it is important to use an APC which will assemble into nanocolumns (rather than nanoparticles) at fast growth rates.

The position of the (Y + RE):Ba:Cu ratio used in all the targets is shown on the phase diagram of figure 1 as a red dot. We show only Y rather than Y + RE on the diagram for simplicity. The target compositions are also listed in table 1 but all have a (Y + RE):Ba:Cu ratio of 1:1.7:2.7, i.e. a target rich in (Y + RE) and Cu compared to YBCO (as can be more easily seen if the composition is normalised to Ba = 2, namely 1.18:2.00:3.18). This ratio was found to be the optimal based on our exploration of cation ratios near to the 1:2:3 ratio, particularly ones which had more Cu or more Y. The 1:1.7:2.7 ratio was found to give the strongest (001) peaks and highest  $T_c$  and  $J_c$  (77 K, self-field) values.

The phase diagram for  $\text{Y}_2\text{O}_3$ -BaO-CuO is shown in figure 1 predicts above the peritectic temperature under reducing oxidation conditions (i.e. above  $\sim 800 \text{ }^\circ\text{C}$  and  $p\text{O}_2 < 0.1 \text{ Torr}$ ). Hence, the 1:1.7:2.7 composition will form a mixture of (Y + RE)BCO, liquid and  $\text{Y}_2\text{BaCuO}_5$  (see blue triangle). However, owing to kinetic factors and epitaxial stabilisation by the forming *c*-aligned (Y + RE)BCO, (Y + RE) $_2\text{O}_3$  forms in the films instead of (Y + RE) $_2\text{BaCuO}_5$  during LAP growth [30]. Hence, the phases which form are those at the vertices of the 'kinetic' tie triangle (shown in red in figure 1), i.e. 1:2:3 + liquid +  $\text{Y}_2\text{O}_3$  (we ignore the (Y + RE) $_2\text{O}_3$  mixed composition, for simplicity here). The position of the liquid phase boundary is not precisely known under the conditions found during growth and is estimated in figure 1. However an approximation of the phase ratios, assuming the positions shown in the 'kinetic' tie triangle of figure 1, gives the mol.% and approximate vol.% (assuming equal volume per atom) of [28, 29] YBCO,  $\text{Y}_2\text{O}_3$  and liquid during the growth to be 88 mol.%, 10 mol.%, 2 mol.%, or 91 vol.%, 3 vol.%, 6 vol.%, respectively.

Differential scanning calorimetry (DSC) measurements were conducted using a TA Instruments Q600 SDT on  $\sim 10 \text{ mg}$  of ground sintered target material. Heating rates of  $15 \text{ min}^{-1}$

were used in a nitrogen atmosphere. The eutectic and peritectic temperatures,  $T_E$ , and  $T_P$ , respectively, were both determined from the DSC measurements (shown in supplementary note 1 (available online at [stacks.iop.org/SUST/34/045012/mmedia](https://stacks.iop.org/SUST/34/045012/mmedia))). This data guided our understanding of the optimum growth temperature to use for the films. The minimum requirement for the LAP process to work is for there to be a liquid present. This means operating marginally above  $T_E$ .

We determined that 820 °C enabled this for all compositions. We note, however, that since the  $T_E$  and  $T_P$  values varied by more than 25 °C across compositions, there would certainly be scope for further individual growth temperature optimisation for each specific composition.

All films are grown using PLD at 820 °C. A Lambda Physik KrF excimer laser was used ( $\lambda = 248 \text{ nm}$ , fluence  $\sim 2 \text{ J cm}^{-2}$ ,  $\sim 0.15 \text{ J pulse}^{-1}$ ) on single crystal (100)  $\text{SrTiO}_3$  (STO) substrates. A laser pulse repetition rate of 50 Hz was used which created a growth rate of  $\sim 250 \text{ nm min}^{-1}$ . This growth rate is higher than standard YBCO PLD film growth by a factor of  $\sim 4\text{--}60$  [27, 31]. The high growth rate is enabled by the presence of a liquid phase in the films during deposition. The growth  $p\text{O}_2$  of all the films was 200 mTorr  $p\text{O}_2$ , and after growth the films were oxygenated at 500 °C in 760 Torr  $p\text{O}_2$  for 1 hour. All films had thicknesses of  $350 \text{ nm} \pm 20 \text{ nm}$ . The deposition temperatures of the films were in the range 750 °C–850 °C, with the temperature of the heater controlled using a conventional thermocouple-P.I.D. controller.

After growing over this range of temperatures, the optimum growth temperature was determined by finding the lowest value of full-width-half-maximum (FWHM) of the (005) x-ray peak, indicative of very high crystalline perfection and the highest  $T_c$  and  $J_c$  (77 K, self-field).

The transition temperature ( $T_c$ ) and the critical-current-density-field dependency ( $J_c(B)$ ) were measured using a conventional four-point probe method. The critical current density measurements used a  $1 \mu\text{V cm}^{-1}$  criterion, the maximum Lorentz force configuration and were conducted on samples etched to have 25  $\mu\text{m}$  wide bridges. The bridges were patterned using a standard photolithographic method with silver electrical contact pads deposited to ensure high quality contact interfaces. After measurement the thicknesses of the films were determined via a Dektak stylus profilometer.

A Philips PW3020 diffractometer employing  $\text{CuK}\alpha$  radiation was used to carry out structural analysis. X-ray diffraction in the Bragg–Brentano geometry and rocking curves of the (005) YBCO peak, (the highest intensity (001) peak), were carried out to study the phases developed in the films and their epitaxial quality. A FEI Nova NanoSEM was also used to create scanning electron microscope images to investigate the surface of the films. Cross-sectional transmission microscopy (TEM) was used to image the BYNO nanoinclusions in the YBCO matrix [25].

### 3. Results and discussion

Table 1 above shows all the compositions studied and information on their structural features,  $T_c$ 's and  $J_c$ 's of the films

**Table 1.** Details of compositions studied, liquid formation temperature, optimum film growth temperatures and  $J_c$  (50 K, 5 T) and (10 K, 10 T). All films were grown at 50 Hz laser repetition rate. Note: the RE ion sizes are  $Y^{3+} = 1.02 \text{ \AA}$ ,  $Yb^{3+} = 0.98 \text{ \AA}$ ,  $Sm^{3+} = 1.09 \text{ \AA}$  [25].

| Sample no.                               | RE:Ba:Cu ratio | RE Composition (Y = 80% + other RE(s) = 20%) | Film Composition acronym     | $T_c$ at optimum growth T $\pm 0.1 \text{ K K}^{-1}$ | c at optimum growth T ( $\text{Å}$ ) | Lowest FWHM of (005) peak in $\theta-2\theta$ | Rocking curve width of (005) peak | $J_c$ (50 K, 5 T)/MA $\text{cm}^{-2}$ | $J_c$ (10 K, 10 T)/MA $\text{cm}^{-2}$ |
|--|----------------|--|------------------------------|--|--------------------------------------|---|-----------------------------------|---------------------------------------|--|
|  |                |  |                              |  |                                      |   |                                   |                                       |  |
| 1  | 1:2:3          | Y  | Y123                         | 79.1   | 11.72                                | 0.369   | 0.348                             | 0.8                                   | 1.4                                    |
| 50 Hz growth high rate (HR) + LAP        |                |  |                              |  |                                      |   |                                   |                                       |  |
| 2  | 1:1.7:2.7      | Y  | Y123 + liquid                | 91.2   | 11.72                                | 0.318   | 0.405                             | 1.7                                   | 4.5                                    |
| 3  | 1:1.7:2.7      | Y, Yb  | (Y,Yb)123 + liquid           | 86.9   | 11.67                                | 0.472   | 0.594                             | 0.8                                   | 3.8                                    |
| 4  | 1:1.7:2.7      | Y, Sm  | (Y,Sm)123 + liquid           | 85.2   | 11.74                                | 0.523   | 0.587                             | 0.9                                   | 4.7                                    |
| 5  | 1:1.7:2.7      | Y, Yb, Sm                                    | (Y,Yb,Sm)123 + liquid        | 88.4   | 11.71                                | 0.427   | 0.542                             | 1.5                                   | 4.3                                    |
| 50 Hz growth high rate (HR) + LAP + BYNO |                |  |                              |  |                                      |   |                                   |                                       |  |
| 6  | 1:1.7:2.7      | Y  | Y123 + liquid + BYNO         | 89.3   | 11.71                                | 0.345   | 0.530                             | 2.1                                   | 4.6                                    |
| 7  | 1:1.7:2.7      | Y, Yb, Sm                                    | (Y,Yb,Sm)123 + liquid + BYNO | 86.6   | 1.71                                 | 0.384   | 0.519                             | 2.0                                   | 7.7                                    |

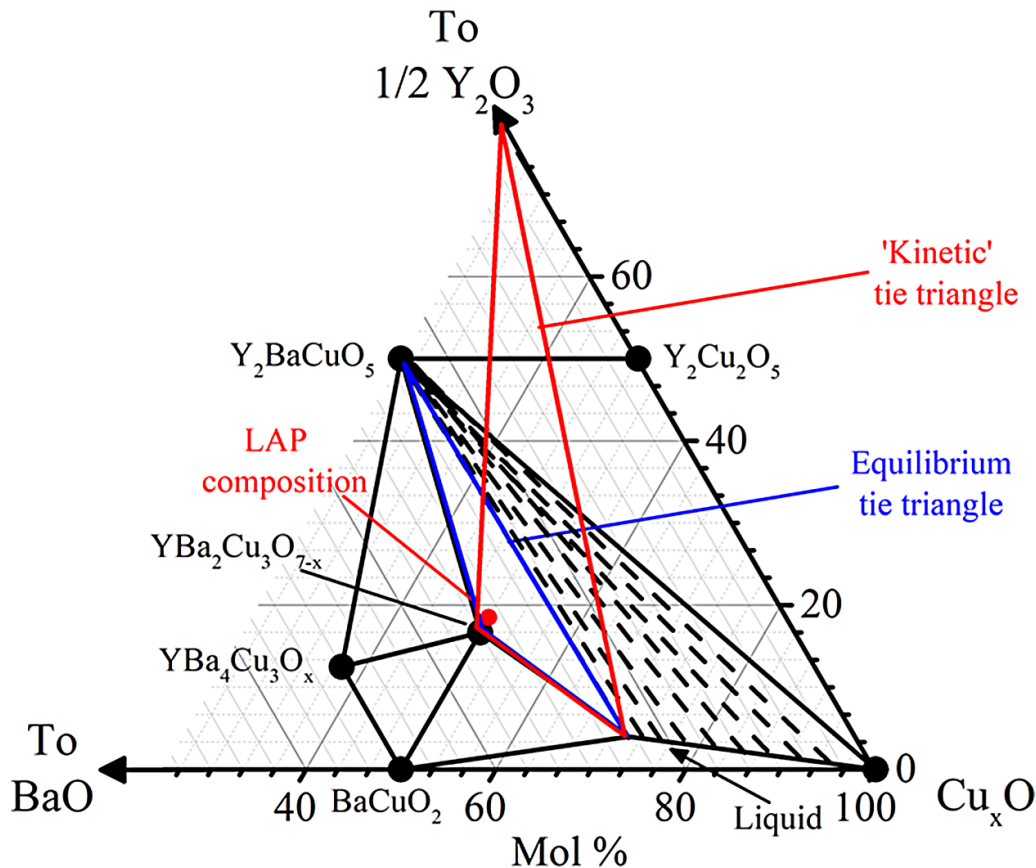


**Figure 1.** Ternary phase diagram of Y-Ba-Cu under a constant low  $pO_2$  ( $<0.1$  Torr.) and temperature of  $800$  °C. Adapted from [28, 29]. Although at equilibrium the phases expected to form are given by the tie triangle around the composition of interest (blue), kinetic and epitaxial growth effects modify this, leading instead to the formation of YBCO, liquid and  $Y_2O_3$  (shown by the red 'kinetic' tie triangle). In this study, some of our compositions have 20% of other REs substituted for Y, but the phase diagram is assumed to be qualitatively the same as for pure Y.

at different  $H$  and  $T$ . As determined from the low FWHM of the (005)  $\theta/2\theta$  and  $\omega$  scans, the films were all highly aligned and had excellent crystallinity, much more so than the plain YBCO film grown at 50 Hz (denoted Y123). As shown in supplementary note 2 (for sample #2 in table 1), the highest  $T_c$  coincided with the lowest level of structural disorder (as determined from the lowest FWHM of the (005) peak) and lowest  $c$  parameter, both indicative of optimum crystalline perfection. This occurred at  $820$  °C, a temperature at which the film growth would be in the presence of liquid at a  $pO_2$  of 200 mTorr. This temperature is higher than typically used during REBCO PLD growth by more than  $30$  °C [32, 33], in order to ensure sufficient liquid is present.

We first consider the reference *stoichiometric* YBCO sample (Y123, sample #1). The film was grown with no liquid present and had a reduced  $T_c$  of 79.0 K. The lower  $T_c$  would be expected for a film grown at very high laser repetition rate (50 Hz) which would be expected to produce a high level of structural disorder [34]. The lower  $T_c$  is also consistent with the non-optimum (too high) growth temperature of  $820$  °C, which is  $\sim 20$  °C– $70$  °C higher than normal for standard YBCO [35]. In contrast, the Y123 + liquid film, #2, has a much higher  $T_c$  of 91.2 K. The higher growth temperature is beneficial as it leads to the formation of liquid in the film, enhancing diffusion kinetics and reducing disorder. Hence,

film #2 has a lower FWHM of the (005) peak than does film #1.

For the RE-added films, the  $c$ -parameter trend follows the pattern expected from the size of the rare-earths, with the (Y,Yb)123 + liquid (#3) film having the smallest  $c$  value (11.67 Å), the (Y,Sm)123 + liquid film (#4) having the largest  $c$  value (11.74 Å) and the (Y,Yb,Sm)123 + liquid film (#5) in between (11.71 Å). The  $T_c$ 's of all the mixed RE films with LAP are lower than pure YBCO with LAP. Of the mixed RE films, the highest  $T_c$  value is for the (Y,Yb,Sm)123 + liquid film (88.4 K), i.e. it is higher than the (Y,Yb)123 + liquid or (Y,Sm)123 + liquid films by up to 3 K. This is likely because the average RE ionic radius in these films (i.e. average of large Sm, middle Y and small Yb) of 1.03 Å is close to the radius of pure Y at 1.02 Å [25], whereas it is either considerably higher or lower for the other compositions.

The  $T_c$ 's for films containing BYNO (i.e. samples #6 and #7, table 1) were slightly lower (by 2 K) than the parent films which did not contain BYNO. This is common for REBCO films that include secondary phases and occurs due to the structural perturbation of the REBCO lattice by the APC [31, 35]. This is manifest as higher FWHM values in the (005) peak in the  $\theta$ - $2\theta$  and  $\omega$  scans, i.e. values of  $\sim 0.34^\circ$  and  $\sim 0.53^\circ$  (#6), respectively. On the other hand, there was only

a marginal effect on the  $c$  parameter, which agrees with a previous study on BYNO doped YBCO [31]. Hence, while there is structural disruption (i.e. buckling of planes and tilting of grains), there is little or no induced cation disorder induced in the REBCO lattice.

Structural disruption in the mixed RE-123 films would be expected to give rise to higher FWHM values for the (005) peaks in the  $\theta$ - $2\theta$  and  $\omega$  scans. We indeed find this to be the case for all the mixed-RE films. The largest structural disorder, lowest  $T_c$  sample, (Y,Sm)123 + liquid (#4) had the largest values of  $\theta$ - $2\theta$  FWHM value of all the films. Compared to the Y123 + liquid film (#2), the FWHM was  $\sim 0.52^\circ$  cf  $\sim 0.32^\circ$ . It also had the largest  $\omega$  scan FWHM value of all the films, i.e.  $\sim 0.59^\circ$  cf  $\sim 0.40^\circ$ , compared to Y123 + liquid sample (#2).

XRD  $\theta/2\theta$  scans of an optimised YBCO films made by the LAP process (i.e. Y123 + liquid, sample #2) is shown in the top half of figure 2(a). The mixed RE films showed very similar patterns in terms of sharp (00l) peaks and similar second phase peaks. The bottom half of figure 2(a) also shows a film made by the LAP process, but now doped with BYNO (i.e. Y123 + liquid + BYNO, sample #6). A clear (400) BYNO peak is observed, as seen in previous BYNO-doped YBCO films [26, 36, 37], indicating that  $c$ -axis oriented BYNO nanocolumns have formed. This was confirmed in cross-sectional TEM images of the films (discussed later). Other phases observed in the x-ray patterns for these films, and all other films grown by the LAP process, are  $Y_2O_3$  + CuO.  $Y_2O_3$  + CuO are phases commonly observed in liquid processed films [14].  $Y_2O_3$  forms due to the excess Y and because it is epitaxially stabilised when YBCO crystallises [28] and CuO forms from the liquid when the film cools after deposition [14].

There was evidence from SEM of the presence of a liquid phase in the LAP films. Figures 2(b) and (c) show example images for sample #2. We see faceted surface secondary-phase particles (figure 2(b)(i)), as well as shallow holes surrounded by very smooth regions (figure 2(b)(ii)). EDX maps (figure 2(c)) confirm the faceted surface particles are Cu-rich (indicative of CuO), and form due to the copper rich composition of the films (as compared to stoichiometric YBCO). The shallow holes seen in the SEM figures arise because of the liquid layer present during deposition in LAP films. Once deposition has finished and the films cool down, the liquid layer solidifies and contracts, leading to the formation of holes and a smooth glassy surface.

We now turn to critical current density ( $J_c$ ) measurements. Figure 3 shows  $J_c$  versus field,  $B \parallel c$  plots for fields up to 11 T at 70 K, 50 K, 30 K and 10 K. We include here all LAP films grown at 50 Hz (#2–#7). We also include the reference 50 Hz YBCO film grown without LAP (Y123, film #1).

First, we observe that the YBCO film grown with LAP at 50 Hz, i.e. film Y123 + liquid (#2), has a considerably higher  $T_c$  and  $J_c$  (by over an order of magnitude at many fields and temperatures) than the stoichiometric YBCO film grown at the same rate but without LAP (#1). The faster diffusion rates available with LAP films would have allowed for a higher quality REBCO crystalline lattice to form, and hence to much less structural perturbation than in the stoichiometric YBCO

film, leading to the much improved  $T_c$  and  $J_c$ . This is a significant result since it is proof that even if point-like disorder is induced by the high growth rates, as might be expected for very-fast-grown stoichiometric YBCO, this alone will not be effective for increasing  $J_c$ . Instead the disorder induced into REBCO (either by fast growth or by mixing REs) needs to be carefully engineered so that the REBCO lattice itself is not perturbed or disrupted to any large extent, in particular in terms of buckling of, or disconnecting, the CuO planes.

Next, we observe in figure 3 that the  $J_c$ 's of the mixed RE films are generally high, and more so with decreasing temperature compared to Y123 + liquid. The high  $J_c$  values for the mixed RE films are exemplified by the '50 K, 5 T' and '10 K, 10 T', values shown in table 1. Hence, introducing liquids into the films enables intrinsic disorder from RE mixing to be effective for pinning even when fast growth rates are used. The benefits of using RE mixing to give high  $J_c$ 's has not been reported before for high rate grown films. This is likely because in the absence of liquids the kinetics are insufficient to 'heal' more long range disorder which is induced from the highly dense atomic disorder associated with the RE1 and RE2 ion size differences in the  $RE_{1-x}RE_2BCO$ .

Looking at the 70 K data first, for samples where the lattice FWHM values are the same, then one would expect the BYNO-added APC films to have superior in-field  $J_c$  because of the positive APC pinning effect. In line with this reasoning, the best performing sample is indeed Y123 + liquid + BYNO (#6). One might then expect the (Y,Yb,Sm)123 + liquid + BYNO film (#7) to be the next in order. However, at this measurement temperature the  $T_c$  of the sample is important: if  $T_c$  is depressed much from 91 K, this will reduce the overall performance. Since the  $T_c$  of #7 is somewhat depressed by the RE mixing, to 86.6 K, the pure Y123 + liquid film (#2) takes the second place slot, with #7 coming third. After this, since there are no further APC doped films, the trend in  $J_c$  then simply reflects the trend in  $T_c$ : i.e. (Y,Yb,Sm)123 + liquid (#5), then (Y,Yb)123 + liquid (#3), then (Y,Sm)123 + liquid (#4) and then Y123 (#1). The strong performance of the Y123 + liquid film in field is most likely due to a population of strong defects such as growth dislocations and twin boundaries, similar to those found in stoichiometric films grown at slow rates [38]. These are expected to be found in all films, but will be disrupted by the high level of OD defects found in RE doped films. We note that any point pinning centres from the RE mixing are easily thermally depinned at this temperature [24] and so produce no benefit.

At 50 K, the (Y,Yb,Sm)123 + liquid + BYNO film (#7) shows a relatively improved performance compared to the 70 K data and now is close to the Y123 + liquid + BYNO (#6) sample despite having a lower  $T_c$  (86.6 K cf 89.3 K). This reveals the strong pinning in this sample from RE mixing effects, over and above the BYNO APC pinning, and the lesser importance of  $T_c$ . The (Y,Yb,Sm)123 + liquid film (#5) also shows a relatively improved performance cf to at 70 K, despite the poorer crystallinity as revealed by the x-ray data, as discussed earlier. Finally, the (Y,Sm)123 + liquid (#4) film rises relative to its respective place at 70 K, although not by as much as #7 and #5. This is likely because both  $T_c$  (86.9 K)

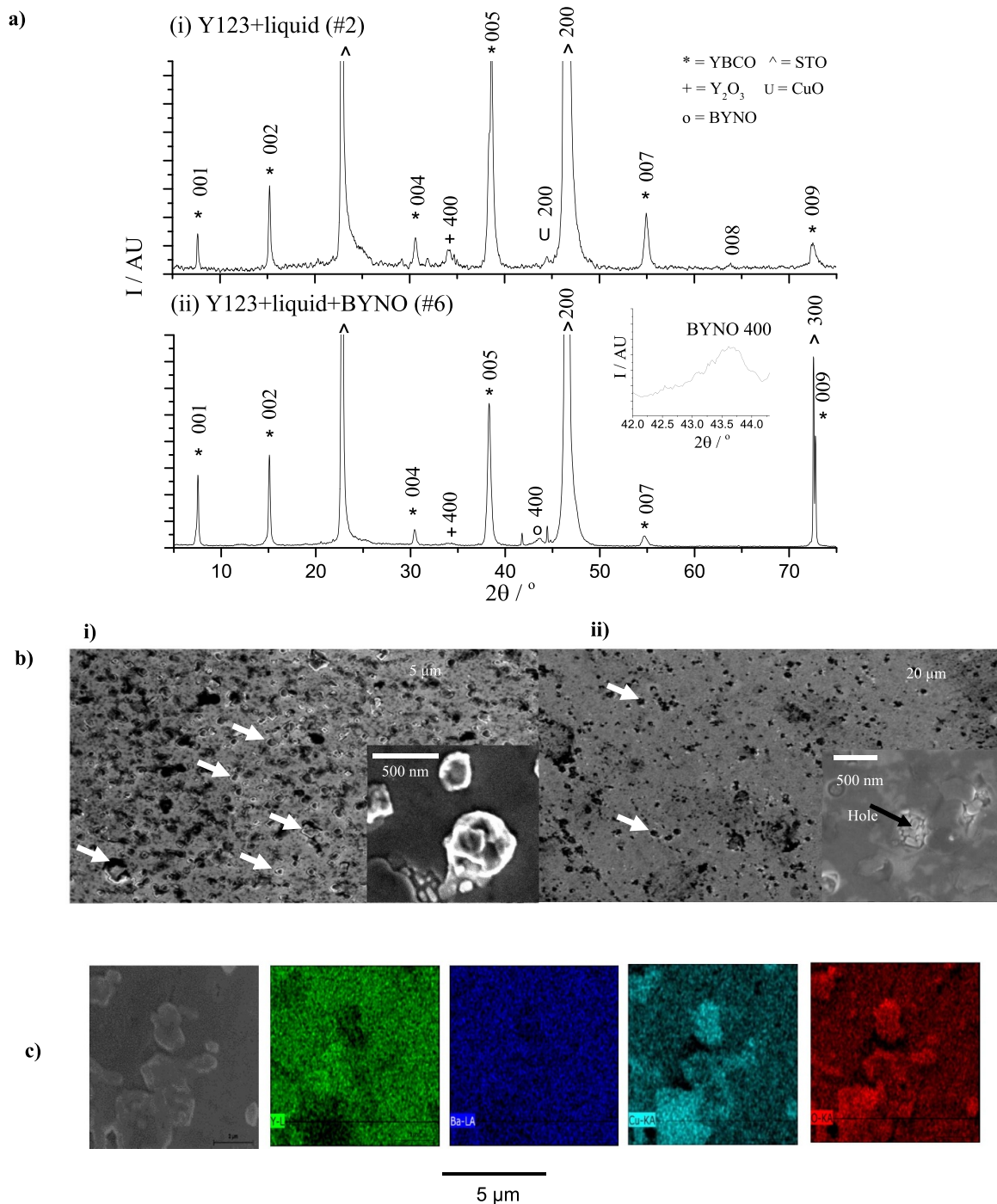


**Figure 2.** Structural and microstructural features of films grown by the LAP process. All films were grown at 820 °C and 50 Hz. (a)  $\theta/2\theta$  traces for (i) film of undoped LAP film (Y123 + liquid, #2) and (ii) BYNO doped LAP film, (Y123 + liquid + BYNO, #6). The  $\theta/2\theta$  labels indicate: \* = (00l) YBCO peaks, + = 004  $RE_2O_3$  peaks, U = (200) CuO peaks, o = (400) BYNO peaks, ^ = (00l) (substrate) STO peaks. Inset shows an enlarged view of the BYNO peak. (b) SEM surfaces images of film #2 showing surfaces features highlighted by arrows (i) round surface particles and (ii) holes (c) EDX mapping revealing the round particles are Cu-rich, indicative of solidified Cu-rich liquid. This liquid is apparent in the phase diagram of figure 1.

and crystallinity are, overall, the worst in sample #4 compared to all the other LAP samples, as shown in table 1.

At 30 K, the Y123 + liquid + BYNO film (#6) continues to perform the best of the samples, indicative of the strong influence of pinning by the nanocolumns. Effective nanocolumnar pinning at 30 K is agreement with what has been found already

for standard REBCO films with APCs [39]. The films with mixed REs show similarly good performance at 30 K of 50 K. Hence, the (Y,Yb,Sm)123 + liquid + BYNO (#7) is nearly as good as the Y123 + liquid + BYNO film (#6). However, the pure Y123 + liquid film (#2) falls further behind of 50 K and 70 K, because it has no APC or point like pinning centres

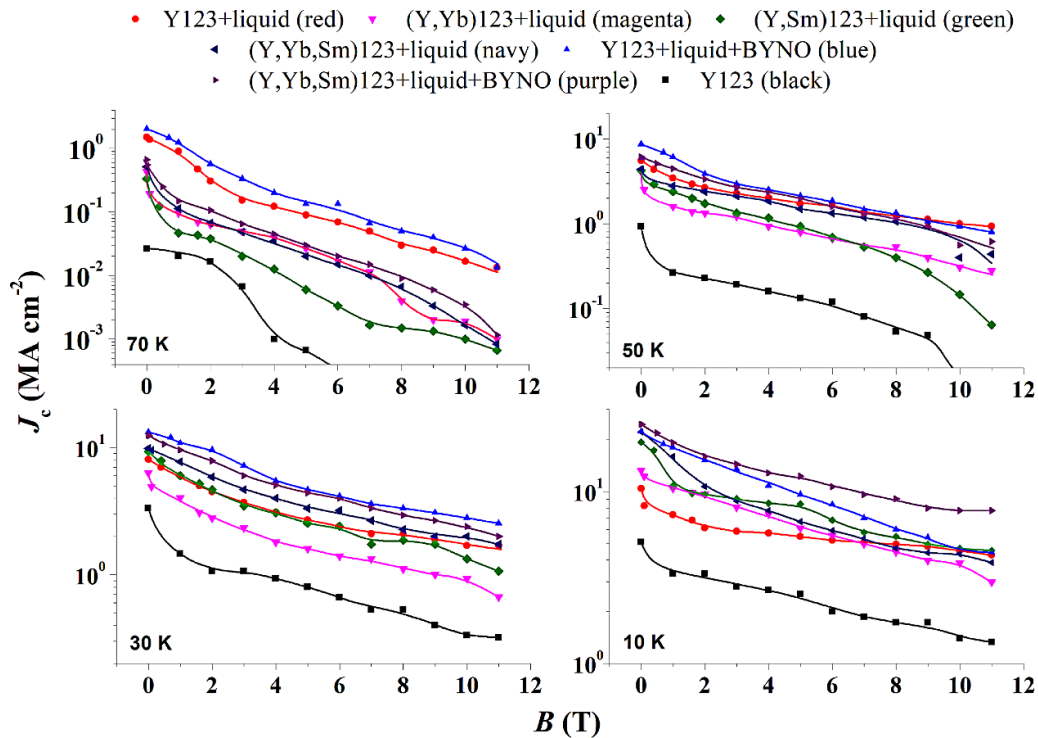


**Figure 3.** Critical current density ( $J_c$ ). Data measured on films deposited at 820 °C and 50 Hz. Film #1: Y123 (black); film #2: Y123 + liquid (red); film #3: (Y,Yb)123 + liquid (magenta); film #4: (Y,Sm)123 + liquid (green); film #5: (Y,Yb,Sm)123 + liquid (navy); film #6: Y123 + liquid + BYNO (blue); film #7: (Y,Yb,Sm)123 + liquid + BYNO (purple). The lines between points are guides for the eye only. The plot shows at least two distinctive regimes present. However, at higher temperatures (70 K and 50 K) three different regions are seen. The first one goes up to  $B_0$ , here between 1 T and 2 T, which is typical for films containing nanocolumns. The second regime is seen as dominated by an exponential decay with an  $\alpha$  exponent given by  $J_c \sim B^{-\alpha}$ . The third regime shows rapid decay of  $J_c$  as the matching field and irreversibility line are approached.

engineered into it. The (Y,Yb,Sm)123 + liquid (#5) is the next best sample, similar to at 50 K. Then, interestingly, compared to at the higher temperatures, (Y,Sm)123 + liquid (#4) swaps its order with (Y,Yb)123 + liquid (#3). This is because the effect of the lower  $T_c$  of #4 is lessened (#4 has the poorest  $T_c$ , 86.9 K, and poorest crystallinity of all the samples) but there are also additional point pins also to be considered as discussed below.

We recall that at 70 K the (Y,Sm)123 + liquid film (#4) had both a worse  $T_c$  and lower  $J_c$  than the (Y,Yb)123 + liquid film (#3), although both are only singly doped with a single non-Y rare-earth. A key difference between these samples is the large  $\text{Sm}^{3+}$  ion size cf. Y. This allows the Sm doped films to develop an extra defect type—the cross substitution of  $\text{Sm}^{3+}$  and  $\text{Ba}^{2+}$  [3, 21]. This does not happen in Yb doped films as the Yb ion size is smaller than Y and there is no cross-substitution with Ba. The cross-substitution point-like defect creates extra disruption reducing the superconducting properties at higher temperatures. However, as the temperature is lowered to 30 K, the defects become effective for pinning as there will not be thermal depinning of this weak defect, as there is at higher temperature. This explains why the  $J_c$  of the (Y,Sm)123 + liquid film rises above that of the (Y,Yb)123 + liquid film at 30 K.

As already noted, while mixed RE films grown in the absence of liquid have not, as far as known, been shown to give rise to effective point pins, this may be because of more long-range disruption of the REBCO lattice when there is no

liquid to ‘heal’ the disruption. Overall, the 30 K data shows that *both* the APCs and RE mixing-related point pinning both play a stronger role in determining  $J_c(B)$  and that at this lower temperature the effect of a reduced  $T_c$  is lessened compared to the higher temperature measurements.

At 10 K, the optimum performing film is (Y,Yb,Sm)123 + liquid + BYNO (#7). It now outperforms Y123 + liquid + BYNO (#6) which was optimum at 30 K. This data further proves that at low temperatures both APC and mixed-RE point like pinning both play strong roles. It also shows that at the lowest temperatures the importance of point pins arising from mixing of REs increases significantly. These point pins provide a weak 0D-like pinning landscape which very effectively supplements the stronger pinning defects arising from the APC columns, leading to very high pinning forces at 10 K, similar to some of the best in the literature, despite the  $\times 4$ –60 faster growth rates.

In terms of the performance of these conductors compared to other liquid processed films grown at similar rates, e.g. an *ex-situ* film made by SuNAM Ltd, the  $J_c$  for films in this study are up to three times higher at 3 T, and six times higher at 5 T [13]. Also, compared to standard stoichiometric YBCO films with  $\text{BaZrO}_3$  and  $\text{Ba}_2\text{Y}(\text{Nb,Ta})\text{O}_6$  pinning additives, the *in situ* LAP films show similar performance over a range of fields from 70 K to 30 K and they outperform these standard APC films at 10 K (by up to a factor of 2), despite being grown 4–60 times faster [27].



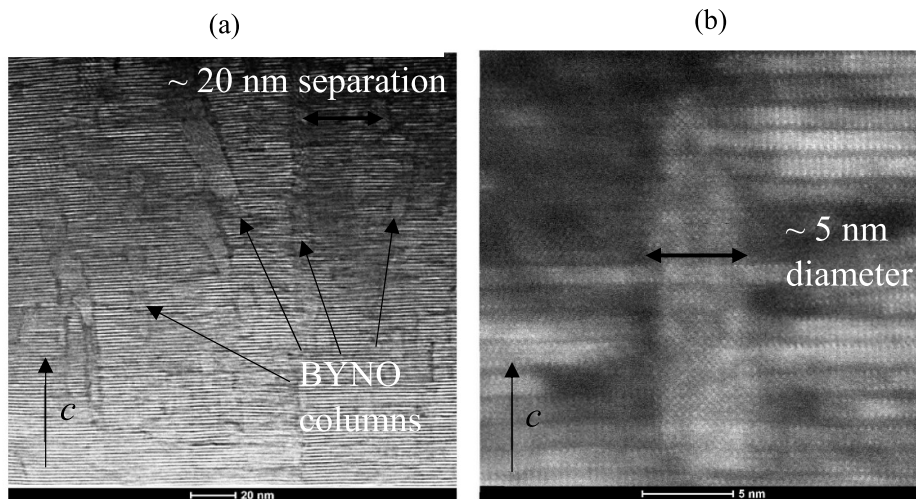


**Figure 4.** Cross sectional TEM images of films showing (a) BYNO columns aligned parallel to  $c$ , spaced  $\sim 20$  nm apart with (b) a diameter of  $\sim 5$  nm.

While it is not possible to image the point-like defects arising from the RE mixing by TEM, it is still important to confirm the nature of the BYNO APC additions to the films which, so far, we have presumed to be columnar owing to the improved  $J_c$  versus  $B \parallel c$ . In figure 4, we show an example of a Y123 + liquid + BYNO LAP film (the same film process as #6). We indeed observe the presence of  $c$ -axis correlated BYNO nanocolumns. Hence BYNO nanocolumns have time to assemble despite the very fast growth rates which typically prevent APCs assembling into well-formed columns [15]. The columns are  $\sim 5$  nm in diameter, spacings  $\sim 20$ – $30$  nm, with  $\sim 40$  nm long segments stacked on top of one another (figure 4(a)). The YBCO lattice between the columns remains highly aligned between the dense, fine columns (as shown in the higher resolution image of figure 4(b)). Although the columns are shorter than the through-thickness columns reported under standard growth conditions for some APCs [35, 38], this is likely not because of a kinetic limitation, but rather because of strain and thermodynamic factors related to BYNO which has a large lattice mismatch with YBCO [15].

The BYNO columns would be expected to act as very strong extended 1D pinning centres for  $B \parallel c$ , explaining the observed behaviour seen in the  $J_c$  measurements. Also, we note that the density of columns is high enough that there are likely to be ‘secondary-effect’ point like defects associated with the columns as they disrupt the REBCO matrix around themselves [15]. This has been effectively seen for MOCVD conductors with 15 at.% BaZrO<sub>3</sub> additions [21].

Finally, we note that while the LAP method demonstrated here for PLD growth could also easily be adapted to other physical or chemical vapour deposition methods to achieve very high-performance conductors at an order of magnitude higher rate, and hence at lower cost.

#### 4. Conclusions

Fast growth of REBCO coated conductors with strong pinning is essential to reduce the cost of superconducting applications.

This paper presents the results of a new *in situ* LAP method that utilises PLD deposition. The method allows for very fast growth rates (up to  $250 \text{ nm s}^{-1}$ ), i.e. more than an order of magnitude faster than standard films. The method enables extended BYNO nanocolumnar APCs to form despite the very fast growth rates, as well as point-like defect pinning centres to be created by having mixed rare-earths in the films. The mixed pinning, mixed RE + BYNO LAP films were shown to be very effective for pinning at 10 K, 30 K and 50 K. Compared to standard YBCO films grown by PLD with different APC pinning additives, despite the much faster growth rates, the LAP films showed similar  $J_c$ 's over a range of fields from 70 K to 30 K, while at 10 K they outperformed the standard films by up to a factor of  $\sim \times 2$ . An increasing influence of point-like pinning from RE mixing in the films at lower temperatures was demonstrated. The LAP method holds much promise for lowering coated conductor cost compared to growth using standard *in situ* vapour growth methods, simply by modifying the composition of the target material.

#### Acknowledgement

The authors thank colleagues who provided figures and feedback on this paper. The authors thank the UK Engineering and Physical Sciences Research Council (EPSRC), Doctoral training account (grant number EP/N509620/1) and SuNAM Co. Ltd. for support and funding. The authors would also like to acknowledge the Henry Royce Institute (Equipment grant ref. EP/P024947/1) for financial support.

#### ORCID iDs

J Feighan <https://orcid.org/0000-0002-5222-7034>

H Wang <https://orcid.org/0000-0002-7397-1209>

J L MacManus-Driscoll <https://orcid.org/0000-0003-4987-6620>

## References

- [1] Obradors X and Puig T 2014 Coated conductors for power applications: materials challenges *Supercond. Sci. Technol.* **27** 044003
- [2] Fietz W *et al* 2013 Prospects of high temperature superconductors for fusion magnets and power applications *Fusion Eng. Des.* **88** 40
- [3] Foltyn S R *et al* 2007 Materials science challenges for high-temperature superconducting wire *Nat. Mater.* **6** 631–42
- [4] Qi X and MacManus-Driscoll J L 2001 Liquid phase epitaxy processing for high temperature superconductor tapes *Curr. Opin. Solid State Mater. Sci.* **5** 291–300
- [5] Kursumovic A *et al* 2000 Study of the rate-limiting processes in liquid-phase epitaxy of thick YBaCuO films *J. Cryst. Growth* **218** 45–56
- [6] MacManus-Driscoll J L 2009 High  $I_c$  in YBCO films grown at very high rates by liquid mediated growth *IEEE Trans. Appl. Supercond.* **19** 3180–3
- [7] Kuphal E 1991 Liquid phase epitaxy *Appl. Phys. A* **52** 380–409
- [8] Hirabayashi I 1995 High  $J_c$  YBCO thick films prepared by LPE method *IEEE Trans. Appl. Supercond.* **5** 2015–8
- [9] Kursumovic A *et al* 2005 High critical current densities in YBa<sub>2</sub>Cu<sub>3</sub>O<sub>7-x</sub> films grown at high rates by hybrid liquid phase epitaxy *Appl. Phys. Lett.* **87** 252507
- [10] Kursumovic A 2004 Hybrid liquid phase epitaxy processes for YBa<sub>2</sub>Cu<sub>3</sub>O<sub>7</sub> film growth *Supercond. Sci. Technol.* **17** 1215–23
- [11] Maiorov B *et al* 2007 Vortex pinning landscape in YBa<sub>2</sub>Cu<sub>3</sub>O<sub>7</sub> films grown by hybrid liquid phase epitaxy *Supercond. Sci. Technol.* **20** 223–9
- [12] Lee J-H *et al* 2014 RCE-DR, a novel process for coated conductor fabrication with high performance *Supercond. Sci. Technol.* **27** 044018
- [13] Lee J *et al* 2016 Enhanced pinning properties of GdBa<sub>2</sub>Cu<sub>3</sub>O<sub>7-δ</sub> coated conductors via a post-annealing process *IEEE Trans. Appl. Supercond.* **26** 8001906
- [14] MacManus-Driscoll J L *et al* 2014 Strong pinning in very fast grown reactive co-evaporated GdBa<sub>2</sub>Cu<sub>3</sub>O<sub>7</sub> coated conductors *APL Mater.* **2** 086103
- [15] Feighan J *et al* 2017 Materials design for artificial pinning centres in superconductor PLD coated conductors *Supercond. Sci. Technol.* **30** 123001
- [16] Rodriguez-Martinez L M *et al* 1996 Cation disorder and size effects in magnetoresistive manganese oxide perovskites *Phys. Rev. B* **54** 622–5
- [17] Radhika Devi A *et al* 2000 Enhanced critical current density due to flux pinning from lattice defects in pulsed laser ablated Y<sub>1-x</sub>Dy<sub>x</sub>Ba<sub>2</sub>Cu<sub>3</sub>O<sub>7-δ</sub> thin films *Supercond. Sci. Technol.* **13** 935–9
- [18] Kwon C *et al* 1999 Fabrication and characterization of (rare-earth)-barium-copper-oxide (RE123 with RE = Y, Er, and Sm) films *IEEE Trans. Appl. Supercond.* **9** 1575–8
- [19] Jia Q X *et al* 2005 Comparative study of REBa<sub>2</sub>Cu<sub>3</sub>O<sub>7</sub> films for coated conductors *IEEE Trans. Appl. Supercond.* **15** 2723–6
- [20] MacManus-Driscoll J L *et al* 2004 Systematic enhancement of in-field critical current density with rare-earth ion size variance in superconducting rare-earth barium cuprate films *Appl. Phys. Lett.* **84** 5329–31
- [21] MacManus-Driscoll J L *et al* 2006 Guidelines for optimizing random and correlated pinning in rare-earth-based superconducting films *Supercond. Sci. Technol.* **19** S55–59
- [22] Wang P F *et al* 2012 Effects of Sm-doping on structures and properties of YBCO coated conductors fabricated by TFA-MOD process *J. Supercond. Nov. Magn.* **25** 261–6
- [23] Jha A K and Matsumoto K 2019 Superconductive REBCO thin films and their nanocomposites: the role of rare-earth oxides in promoting sustainable energy *Front. Phys.* **7** 82
- [24] Puig T 2008 Vortex pinning in chemical solution nanostructured YBCO films *Supercond. Sci. Technol.* **21** 034008
- [25] MacManus-Driscoll J L 1994 Studies of structural disorder in ReBa<sub>2</sub>Cu<sub>3</sub>O<sub>7-x</sub> thin films (Re = rare earth) as a function of rare-earth ionic radius and film deposition conditions *Physica C* **232** 288–308
- [26] Ercolano G *et al* 2014 Strong correlated pinning at high growth rates in YBa<sub>2</sub>Cu<sub>3</sub>O<sub>7-x</sub> thin films with Ba<sub>2</sub>YNbO<sub>6</sub> additions *APL Mater.* **116** 033915
- [27] Celentano G *et al* 2020 YBa<sub>2</sub>Cu<sub>3</sub>O<sub>7-x</sub> films with Ba<sub>2</sub>Y(Nb,Ta)O<sub>6</sub> nanoinclusions for high-field applications *Supercond. Sci. Technol.* **33** 044010
- [28] Poole C 2000 *Handbook of Superconductivity* (New York: Academic)
- [29] Macmanus-Driscoll J L 2004 Materials chemistry and thermodynamics of REBa<sub>2</sub>Cu<sub>3</sub>O<sub>7-x</sub> *Adv. Mater.* **9** 457–73
- [30] Ohnishi T *et al* 2004 High rate *in situ* YBa<sub>2</sub>Cu<sub>3</sub>O<sub>7</sub> film growth assisted by liquid phase *J. Mater. Sci.* **19** 977–81
- [31] Ercolano G *et al* 2010 Enhanced flux pinning in YBa<sub>2</sub>Cu<sub>3</sub>O<sub>7-δ</sub> thin films using Nb-based double perovskite additions *Supercond. Sci. Technol.* **23** 022003
- [32] Greer J A 1992 High quality YBCO films grown over large areas by pulsed laser deposition *J. Vac. Sci. Technol.* **10** 1821–6
- [33] Gupta A *et al* 1990 Defect formation caused by a transient decrease in the ambient oxygen concentration during growth of YBa<sub>2</sub>Cu<sub>3</sub>O<sub>7-δ</sub> films *APL Mater.* **57** 2365–7
- [34] Suh J D and Sung G Y 1997 Crystal orientation control of YBa<sub>2</sub>Cu<sub>3</sub>O<sub>7-x</sub> thin films prepared by pulsed laser deposition *Physica C* **282** 579–80
- [35] Harrington S A *et al* 2008 Self-assembled, rare earth tantalate pyrochlore nanoparticles for superior flux pinning in YBa<sub>2</sub>Cu<sub>3</sub>O<sub>7-δ</sub> films *Supercond. Sci. Technol.* **22** 022001
- [36] Wee S *et al* 2010 Formation of self-assembled, double-perovskite, Ba<sub>2</sub>YNbO<sub>6</sub> nanocolumns and their contribution to flux-pinning and  $J_c$  in Nb-doped YBa<sub>2</sub>Cu<sub>3</sub>O<sub>7</sub> films *Appl. Phys. Express* **3** 023101
- [37] Opherden L *et al* 2016 Large pinning forces and matching effects in YBa<sub>2</sub>Cu<sub>3</sub>O<sub>7-δ</sub> thin films with Ba<sub>2</sub>Y(Nb/Ta)O<sub>6</sub> nano-precipitates *Sci. Rep.* **6** 21188
- [38] Xu A *et al* 2014 Strongly enhanced vortex pinning from 4 to 77 K in magnetic fields up to 31 T in 15 mol.% Zr-added (Gd, Y)-Ba-Cu-O superconducting tapes *APL Mater.* **2** 046111
- [39] Haberkorn N *et al* 2012 High-temperature change of the creep rate in YBa<sub>2</sub>Cu<sub>3</sub>O<sub>7-δ</sub> films with different pinning landscapes *Phys. Rev. B* **85** 174504